

Deactivation and Regeneration of Ni Catalyst During Steam Reforming of Model Biogas: An experimental investigation

Srinivas Appari^a, Vinod M. Janardhanan^{a,1}, Ranjit Bauri^b, Sreenivas Jayanti^c

^aDepartment of Chemical Engineering, Indian Institute of Technology Hyderabad, Andhra Pradesh 502 205, India

^bDepartment of Metallurgical and Materials Engineering, Indian Institute of Technology Madras, Chennai 600 036, Tamil Nadu, India

^cDepartment of Chemical Engineering, Indian Institute of Technology Madras, Chennai 600 036, Tamil Nadu, India

Abstract

This paper presents detailed study of biogas reforming. Model biogas with different levels of H₂S is subjected to reforming reaction over supported Ni catalyst in a fixed bed reactor at 700 °C and 800 °C. In order to understand the poisoning effects of H₂S the reactions have been initially carried out without H₂S in the feed stream. Three different H₂S concentrations (20, 50 and 100 ppm) have been considered in the study. The H₂O to CH₄ ratio is maintained in such a way that CO₂ also participates in the reforming reaction. After performing the poisoning studies, regeneration of the catalyst has been studied using three different techniques i) removal of H₂S from the feed stream ii) temperature enhancement and iii) steam treatment. Poisoning at low temperature is not recoverable just by removal of H₂S from the feed stream. However, poisoning at high temperature is easily reversed just by removal of H₂S from the feed stream. Unlike some previous reports [1, 2], catalyst regeneration is achieved in shorter time frames for all the regeneration techniques attempted.

Keywords: Biogas, Steam Reforming, Catalyst Poisoning, Kinetics, Deactivation, Regeneration

1. Introduction

Bio-gas is an alternate fuel for synthesis gas production containing 50-75% CH₄, 50-25% CO₂, 0-10% N₂, and 0-3% H₂S. Due to the trivial nature of the anaerobic digestion process by which it is produced it can serve as a decentralized source of energy. The bio-gas thus produced can be converted into synthesis gas either by dry reforming or by a combination of dry and steam reforming using appropriate catalysts [3, 4]. Since the CH₄ to CO₂ ratio in bio-gas is ~1.5, dry reforming alone can lead to significant carbon deposition within the reactor [5]. Therefore, it is desirable to mix bio-gas with steam for reforming and generally the H₂O to CH₄ ratio (S/C) is maintained at 3 to avoid any coke formation [6].

Biogas is an ideal gas for distributed power generation using Solid-Oxide Fuel Cells (SOFC), especially in areas that are not grid connected. The most interesting aspect of biogas fueled high temperature fuel cell system for power generation is the carbon neutral cycle. Although high temperature fuel cells such as SOFC can operate on hydrocarbon fuels without upstream fuel processing [7], in most cases the target fuel is either fully or partially reformed in an upstream fuel processor [8]. In an SOFC plant the fuel processor is connected to the SOFC stack with appropriate heat exchange and steam mixing. However, one of the major challenges in utilizing bio-gas for SOFC application is presence of H₂S. H₂S present in the bio-gas easily

deactivates Ni which is conventionally used in the anode of SOFCs. H₂S content in the feed gas can be reduced by employing a desulfurization unit, however, this is economically less attractive for small scale distributed power generation using SOFCs.

There are several reports that investigate steam reforming of biogas [9, 10, 3]. However, these studies do not account for the presence of H₂S, which is generally present in biogas. Biogas reforming without desulfurization will lead to catalyst deactivation due to sulfur poisoning. Sulfur poisoning of Ni and Pt has been studied widely, however, most of the transition metals lose catalytic activity in presence of H₂S and other sulfur containing compounds [11]. Generally the deactivation of reforming catalyst is exponential in time and deactivation times ranging from 5 to 20 hours have been reported using time on stream analyses [12, 13]. The deactivation rate is faster when the H₂S concentration is higher [13]. However, there are also reports which show a precipitous drop in the activity of the Ni catalyst on exposure to H₂S [1].

The objective of this work is to study the deactivation and regeneration of Ni catalyst supported on γ -Al₂O₃ (Ni/ γ -Al₂O₃) during steam reforming of biogas containing ppm levels of H₂S. Although several studies have been reported on the poisoning effect of sulfur on transition metal catalysts, majority of them have been performed using H₂S diluted in H₂ or CO and H₂O [14, 12, 15, 16]. Studying the poisoning effect of H₂S on catalytic surface during reforming of hydrocarbon is more complex due to the competition among various molecules and

Email address: vj@iith.ac.in, Tel: +91 (0) 40 2301 6073,
Fax: +91(0) 40 2301 6032 (Vinod M. Janardhanan)

radicals for active sites. For instance the saturation coverage of H atoms on a catalytic surface is significantly affected by the partial pressure of CO in the gas mixture. To the best of our knowledge, the report by Ashrafi et al. [13] is the only one that addresses the time on stream effect of H₂S during the steam reforming of biogas. Although not dealing with biogas, another report that looks into the effect of sulfur during the steam reforming of CH₄ is by Li et al. [1]. However, this study contradicts with the report of Ashrafi et al. According to Li et al. deactivation of Ni/ γ -Al₂O₃ due to H₂S is instantaneous and the regeneration is a slow process, whereas according to Ashrafi et al. both deactivation and regeneration are slow processes. Nevertheless, the major focus of the work by Li et al. is regeneration methods. According to them, the conventional regeneration methods such as sequential steam, steam-air, steam-hydrogen treatment, and high temperature reaction treatment are ineffective in completely recovering the catalyst activity. Interestingly, in their report the reforming activity of the regenerated catalyst using the conventional method is not stable and falls over time on stream. In the present work, we study the kinetics of deactivation and subsequent regeneration of the catalyst, focusing primarily on the effect of concentration of H₂S and the temperature at which the deactivation and regeneration take place.

2. Experimental details

2.1. Catalyst preparation

Initially the γ -Al₂O₃ (Alfa Aesar) supports (pellets of average length = 5.1 mm and average diameter = 3.3 mm) are calcined in air at 800 °C and held for 4 hr to remove any volatile components present. The nickel metal catalysts supported on γ -Al₂O₃ are prepared by wet impregnation method using nickel (II) nitrate hexahydrate (Merck, 99% purity) as precursor. Measured quantities of metal precursor equivalent to the desired metal loading (15 wt%) are first dissolved in distilled water of volume equal to or slightly in excess of the total pore volume of the support. The required amount of γ -Al₂O₃ pellets is then added to the precursor solution and stirred continuously for two hours to ensure that the precursor solution is uniform during the wet impregnation process. The wet materials are subsequently dried overnight at 80 °C followed by calcination at 800 °C in presence of air for 6 h.

2.2. Catalyst characterization

XRD (X-Pert PRO PAN analytical) analysis is conducted for catalyst samples between $2\theta = 10^\circ$ to 90° using CuK α radiation ($\lambda=0.15418$ nm) at 40 kV and 30 mA. Figure 1 shows XRD patterns of pure γ -Al₂O₃, calcined Ni/ γ -Al₂O₃, reduced Ni/ γ -Al₂O₃, spent catalyst at 800 °C after stability test without H₂S exposure, and spent catalyst at 700 °C exposed to 100 ppm H₂S. The presence of NiO is confirmed for calcined Ni/ γ -Al₂O₃ at angles of 37.3° and 66.1° , and an inactive NiAl₂O₄ crystalline phase at 45.6° . The formation of NiAl₂O₄ is due to the higher calcination temperature (800 °C). The Ni peaks are observed at 44.6° , 51.9° and 76.4° degrees for reduced

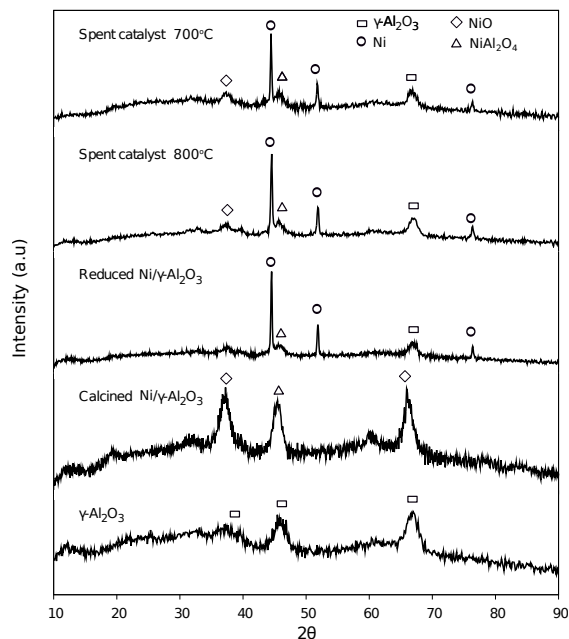


Figure 1: XRD patterns of Ni, NiO, NiAl₂O₄ and γ -Al₂O₃. The phases are denoted by symbols.

catalyst and spent catalyst at 800 °C and 700 °C. Reduced Ni/ γ -Al₂O₃ and spent catalysts at 700 °C and 800 °C showed lower peak intensity for NiAl₂O₄, which is in good agreement with previous literature [17]. The diffraction patterns for NiS and Ni₃S₂ are not observed for the spent catalyst at 700 °C with 100 ppm H₂S exposure even though the catalyst is almost fully poisoned. A similar XRD pattern was observed by Kuhn, et al. [18], for Ni-YSZ sample exposed to 100 ppm H₂S. The absence of stable compounds of NiS or Ni₃S₂ in the XRD pattern is not surprising as these are expected to form only at high concentrations of H₂S in the feed. For low concentrations (<100 ppm), it is thought that the formation of chemisorbed S on Ni leads to deactivation [18]. The diffraction peak for graphite carbon at 26.50° is not observed for spent catalyst at 700 °C and 800 °C. γ -Al₂O₃ showed poor intensity for all the catalysts as shown in Fig. 1 at angles of 37.8° , 45.4° and 67.2° degrees.

The BET surface area, pore size distribution and average pore diameter of the catalysts are measured using Micromeritics ASAP 2020 surface and porosity analyzer. In order to remove the moisture and any adsorbed gases, the samples are degassed under vacuum for 6 h at 200 °C. The pore size distribution is calculated from N₂ desorption data using the Barrett-Joyner-Halenda (BJH) method. The BET surface area of calcined γ -Al₂O₃, reduced catalyst, and spent catalysts are shown in Table 1. The surface area of γ -Al₂O₃ calcined at 800 °C is $206 \text{ m}^2\text{g}^{-1}$. The calcined and reduced catalysts showed lower surface area compared to γ -Al₂O₃, probably due to pore blockage. The reduced catalyst showed lower surface area compared to calcined sample due to the agglomeration of Ni particles at higher reduction temperature. The BET surface area for spent catalysts is significantly lower than that of fresh samples.

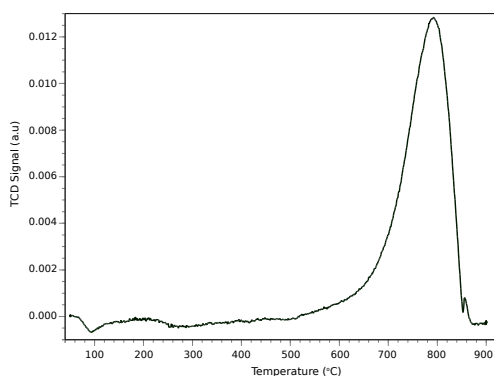


Figure 2: TPR Profile for 15% Ni/ γ Al₂O₃ calcined at 800 °C.

The temperature programmed reduction (TPR) studies have been carried out using Micrometrics AutoChem II-2920 chemisorption analyzer. A measured amount of fresh catalysts is loaded in U shaped quartz tube and heated to 200 °C for 1 hr in Ar stream (30 ml min⁻¹). The samples are then cooled down to 50 °C and the Ar is replaced by 10 vol% H₂ in Ar (30 ml min⁻¹). The samples are heated from 50 °C to 900 °C at a ramp rate of 10 °C per min. The consumption of H₂ is monitored using a thermal conductivity detector (TCD). Figure 2 shows that maximum degree of reduction occurs at 790 °C. The higher reduction temperature indicates the strong interaction of NiO with γ -Al₂O₃ support. The higher calcination temperatures may also result in the formation of NiAl₂O₄ and the broad reduction peak may also be due to the reduction NiAl₂O₄.

To determine the active metal surface area, metal dispersion, and average metal particle size, H₂ pulse chemisorption studies have been carried out using Micrometrics AutoChem II- 2920 chemisorption analyzer. Measured amount of fresh catalysts is loaded in a quartz tube and reduced with 10 vol.% H₂ in Ar (30 ml min⁻¹). After reduction the sample is cooled down to 50 °C and Ar flow is continued for another 30 min to remove traces of H₂. Following this several pulses of measured quantity of 10 vol.% H₂ in Ar are introduced into the reduced catalyst sample until three consecutive similar H₂ peaks are obtained. H₂ pulse chemisorption results for Ni/ γ -Al₂O₃ reduced at temperature of 800 °C for 15 wt% Ni loading gave 3% metal dispersion, metallic surface area of 19.9 m²g⁻¹, and cubic crystallite size of 28.1 nm. This particle size is very close to the value calculated using Scherrer equation, which gives 34.2 nm.

2.3. Steam reforming experiments

Biogas steam reforming experiments were carried out in a fixed bed quartz reactor (20 mm outside diameter and 1 mm wall thickness) maintained at atmospheric pressure. The reactor loaded with 1.5 gm of catalyst pellets diluted with quartz beads (3 mm to 5 mm diameter) was placed in a three zone heating furnace (Applied Test Systems, INC, USA). The catalytic bed was placed in the quartz tube reactor using quartz

wool. A schematic representation of the reactor is shown in Fig. 3. The reactor was heated to the desired temperature at a rate of 10 °C per min under N₂ flow (99.999% pure, Prax air). Furnace temperature was adjusted to maintain the catalyst bed under isothermal condition. K-type thermocouples were used to measure the reactor temperature. Two Ni-Cr thermocouples were placed at the top and bottom of the catalytic bed to measure the catalyst bed temperature. Prior to the reactions the catalysts were reduced in pure H₂ flow (20 mL min⁻¹) at 800 °C for 5 hours. Before starting the reaction, water was fed using a calibrated HPLC pump (LabAlliance, USA) through a preheater to the reactor for 5 mins. Pure gases of CH₄ (99.999%) and CO₂ (99.995%) were fed to the reactor using calibrated mass flow controllers (Bronkhorst High Tech, The Netherlands) with N₂ dilution. The gas mixture was heated to 250 °C in a preheat-

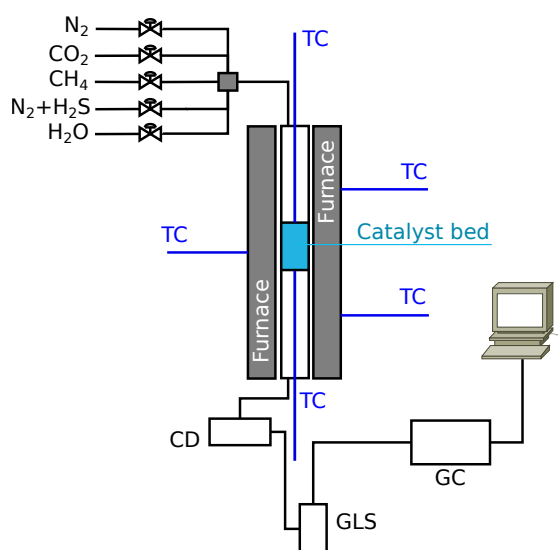


Figure 3: A schematic representation of reactor used for experiments. The abbreviations used are as follows: Thermocouple (TC), Gas-Liquid separator (GLS), Condenser (CD), Gaschromatograph (GC)

ing zone before entering the reactor hot zone. Water present in the reactor exhaust was condensed using a condenser and gas-liquid separator (GLS). The condenser and GLS were maintained at 0 °C by using a chiller (Zulabo, Germany). The dry gasses were analyzed using online GC 2014 (Shimadzu Corporation) equipped with TCD in a carboxane packed column (inner diameter 3.17 mm and length 4.5 m). The biogas steam reforming reaction was performed until steady state and up on reaching the steady state H₂S was introduced into the reactor from a cylinder containing H₂S diluted in N₂. The reforming reactions were continued in the presence of H₂S and sampling was done for every 15-30 min until a new steady state. Three different techniques have been explored for catalyst regeneration

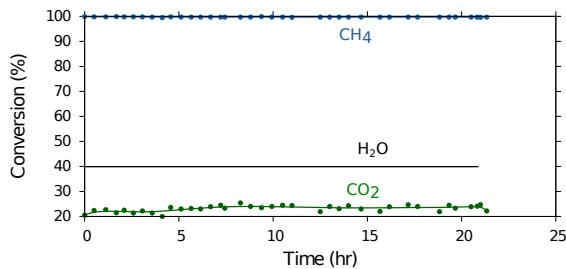
- removal of H₂S from feed stream
- temperature enhancement
- steam treatment

All the experiments were repeated to ensure reproducibility.

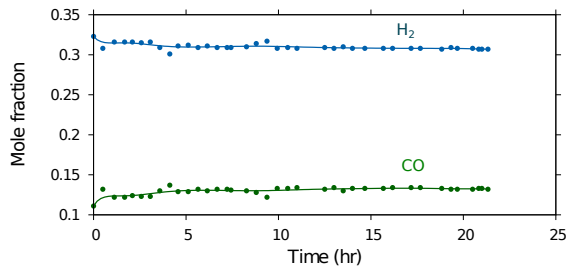
3. Results and discussion

3.1. Stability tests

Before introducing H_2S to the system to study the deactivation at different H_2S concentrations and temperatures, the biogas steam reforming reactions are performed without H_2S and held at least for 1 hr at steady state. H_2S is then introduced from an N_2 cylinder containing 1052 ppm H_2S . CH_4 (23.8 ml min^{-1}), CO_2 ($15.99 \text{ ml min}^{-1}$), N_2 ($102.4 \text{ ml min}^{-1}$), and H_2O ($48.08 \text{ ml min}^{-1}$) are introduced to the reactor. This corresponds to CH_4 to CO_2 ratio of 1.487 and H_2O to CH_4 ratio (S/C) of 2.02. The corresponding inlet mole fractions are $CH_4 = 0.125$, $CO_2 = 0.084$, $H_2O = 0.252$ and $N_2 = 0.539$. A low S/C ratio is employed to ensure the participation of CO_2 in reforming reactions [9]. Nevertheless, it is worth mentioning here that S/C ratio may have some influence on the chemisorption equilibrium of H_2S at temperatures above $700 \text{ }^\circ\text{C}$ [2].



(a) Time on stream conversion of H_2O , CH_4 and CO_2 during catalyst stability test at $800 \text{ }^\circ\text{C}$



(b) Time on stream mole fraction of H_2 and CO during catalyst stability test at $800 \text{ }^\circ\text{C}$

Figure 4: Conversions of CH_4 and CO_2 during stability test at $800 \text{ }^\circ\text{C}$ and the corresponding mole fractions of H_2 and CO in the products

In order to ensure that the catalyst does not lose activity over time in non poisoning atmosphere (without H_2S) reforming experiments are performed for 22 hrs at $800 \text{ }^\circ\text{C}$. Figure 4(a) shows the conversion of CH_4 and CO_2 on dry basis and H_2O conversion during the catalyst stability test at $800 \text{ }^\circ\text{C}$. All data reported in this paper is on dry basis and the lines are just drawn to guide the eye. The reactor exit compositions for the stability test are shown in Fig. 4(b). The constant conversion and product composition implies that the catalyst is

stable and the activity remains constant under non-poisoning gas atmosphere. The H_2 to CO ratio in the product gas for the given inlet composition is ~ 3 . The stability test is also carried out at $700 \text{ }^\circ\text{C}$. The H_2 to CO ratio at $700 \text{ }^\circ\text{C}$ is ~ 2.72 and CO_2 conversion is lower compared to $800 \text{ }^\circ\text{C}$, which can be attributed to the shifting of the thermodynamic equilibrium of the reactions involved. Table 2 shows a comparison between equilibrium predictions and the experimental data. The equilibrium composition is calculated using the software DETCHEM by considering CH_4 , H_2 , CO , CO_2 , H_2O and N_2 in the mixture [19]. It can be seen that the conversions and product mole fractions agree well with the equilibrium calculations. Since all the catalysts used in the experiments are prepared in the same batch and since they are stable under non-poisoning gas atmosphere, we can assert that the catalyst deactivation by introducing H_2S to the feed gas is purely due to sulfur poisoning, at least for the time on stream considered in this study.

3.2. Deactivation studies

Catalyst deactivation experiments are performed for two different temperatures and three different H_2S concentrations. Figure 5 shows the deactivation of the catalyst for 20, 50, and 100 ppm H_2S with respect to CH_4+CO_2 concentration at $700 \text{ }^\circ\text{C}$. All H_2S concentrations led to almost complete deactivation (98%) of the catalyst, however, the rate at which deactivation occur varies. Higher H_2S concentrations lead to faster deactivation. Figure 6 shows drop in CH_4 conversion as a result of deactivation at $800 \text{ }^\circ\text{C}$ for different H_2S concentrations. In all cases the catalyst activity dropped, however, did not deactivate fully. The residual activity retained by the catalyst depends on the concentration of H_2S in the feed gas. 100 ppm H_2S concentration in the feed gas led to a final steady state of 34% CH_4 conversion, 50 ppm to 43%, and 20 ppm to 48%. Deactivation rate for 10, 50, and 100 ppm for the two temperatures may also be inferred by comparing Fig. 5 and Fig. 6. It is interesting to notice that for both the temperatures the rate of activity loss (the slope of the curve) before reaching steady state is same for 50 and 100 ppm whereas for 20 ppm the rate of deactivation is much slower at $800 \text{ }^\circ\text{C}$ compared to $700 \text{ }^\circ\text{C}$. For both the temperatures CH_4 conversion is $\sim 98-99\%$ in the absence of H_2S in the feed gas. Therefore, the catalyst deactivation is purely due to sulfur poisoning. The H_2 and CO mole fractions from the

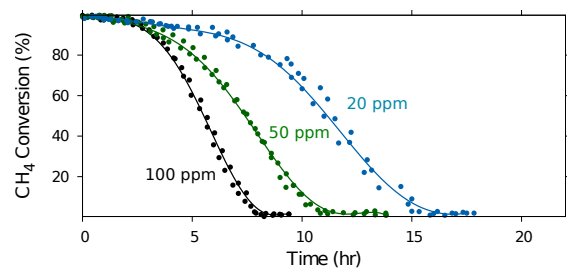


Figure 5: CH_4 conversion at $700 \text{ }^\circ\text{C}$ as a function of time for three different H_2S concentrations.

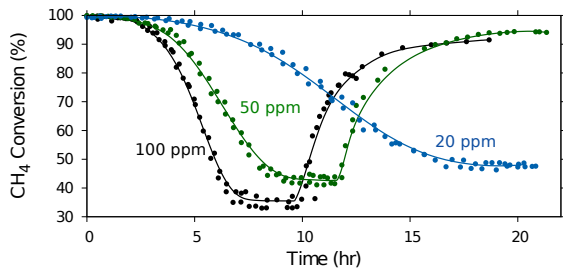
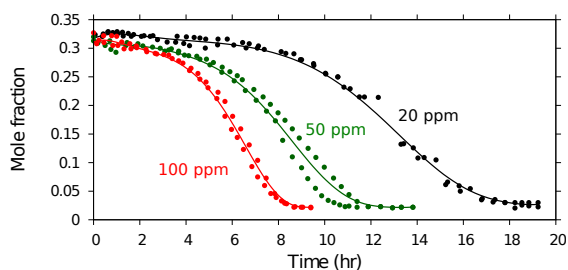
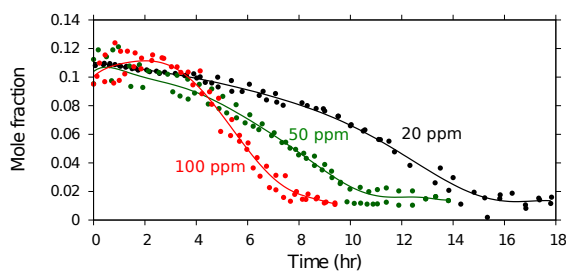


Figure 6: CH₄ conversion at 800 °C as a function of time for three different H₂S concentrations. For 100 ppm H₂S is removed at 8 hrs 40 min and the regeneration is continued until 17 hrs 40 min. For 50 ppm H₂S is removed at 11 hrs 20 min and the regeneration is continued till 21 hrs.

reactor exit at 700 °C during deactivation for different H₂S concentrations are shown in Fig. 7. Examining Fig. 5 and Fig. 7 leads us to the conclusion that the final activity of the catalyst is independent of the H₂S concentration. In all cases the catalyst retained ~2% of its activity. However, the same is not true for high temperature operation. Fig. 8 shows the exit mole fractions of H₂ and CO at 800 °C. Higher ppm level of H₂S results in low CH₄ conversion and hence low H₂ mole fraction in the product stream. That is at low operating temperatures, the saturation coverage of sulfur on Ni is independent of H₂S concentration. All the H₂S concentrations considered in this study lead to saturation coverages at 700 °C whereas at high temperature, the mechanistic of H₂S adsorption and recombination reaction involving sulfur leads to different saturation coverages of sulfur for different H₂S concentrations.



(a) H₂ mole fraction from the reactor exit at 700 °C



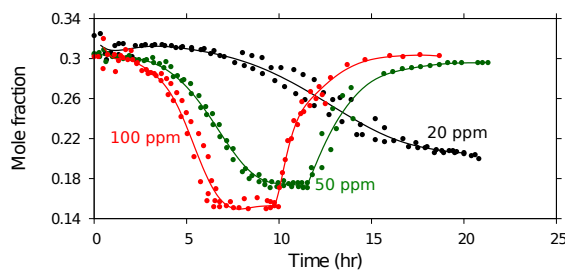
(b) CO mole fraction from the reactor exit at 700 °C

Figure 7: H₂ and CO mole fraction at the reactor exit for different H₂S concentrations at 700 °C

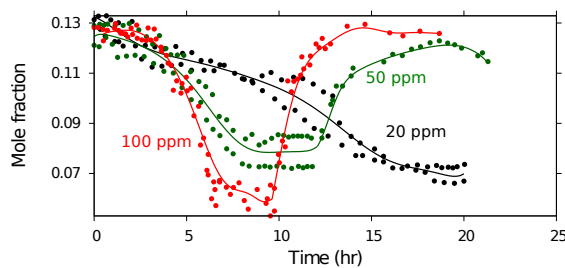
3.3. Regeneration by H₂S removal

Since chemisorption is a reversible process, surface adsorbed sulfur can be removed by decreasing the sulfur content in the

feed stream [2]. For 100 and 50 ppm we have performed the regeneration experiments by removing H₂S from the feed gas (all other gas flow rates remain the same) after reaching their steady state residual activity. For both 100 and 50 ppm the catalyst activity again reached another steady state after H₂S removal (Fig. 6). However, full regeneration could not be achieved. In the case of 50 ppm 95% activity could be recovered, whereas for 100 ppm recovery is only 90%. The time required for regeneration is ~10 h, which is very short compared to the time required for conventional regeneration methods reported by Li et. al [1]. We could not perform regeneration experiments for 20 ppm due to periodic power outages after every 24 hrs. The rate of regeneration is same as rate of deactivation in all cases. For instance from Fig. 6 the deactivation for 100 ppm H₂S takes about 8 hrs and the regeneration also takes approximately the same duration. These results are consistent with the report of Ashrafi et al [13]. The catalyst activity loss is mainly due to dissociative adsorption of H₂S on Ni leading to the active sites being covered with sulfur. At high temperature each sulfur atom occupies one adsorption site on Ni [14]. To recover the activity the adsorbed sulfur needs to be removed from the active sites of the catalyst. The surface adsorbed sulfur can participate in recombination reactions with a number of other surface adsorbed species such as H, O, and OH. The recombination products can then desorb from the surface, leaving the surface again capable of promoting surface reactions. The partial recovery of activity would then imply that the adsorbed sulfur is not fully removed by the recombination reactions.



(a) H₂ mole fraction from the reactor exit at 800 °C



(b) CO mole fraction from the reactor exit at 800 °C

Figure 8: H₂ and CO mole fraction at the reactor exit for different H₂S concentrations at 800 °C. For 100 ppm H₂S is removed at 8 hrs 40 min and the regeneration is continued until 17 hrs 40 min. For 50 ppm H₂S is removed at 11 hrs 20 min and the regeneration is continued till 21 hrs.

3.4. Regeneration by temperature enhancement

At 800 °C the catalyst activity is recovered by removing H₂S from the feed gas. However, at 700 °C the catalyst activity could not be recovered in the same manner. This means that the kinetics of desorption and/or recombination reactions are not favored at low temperatures. This is further confirmed by temperature stepping at 700 °C which lead to recover the activity. Figure 9 shows the gain in catalytic activity when the temperature is increased from 700 °C to 800 °C. 100 ppm H₂S concentration at 700 °C leads to almost complete deactivation of the catalyst. However, when the temperature is increased to 800 °C, the catalyst started regaining activity and stabilizes at 32% CH₄ conversion, very close to the steady state activity at 800 °C for 100 ppm reported in Fig. 6. This

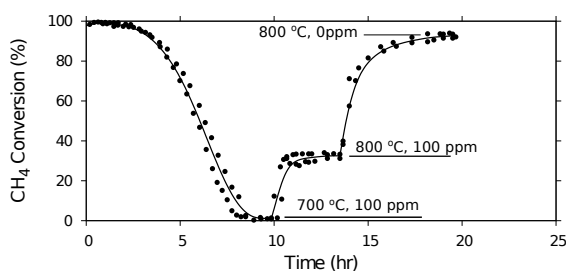


Figure 9: Effect of temperature and H₂S concentration on regaining catalyst activity. Temperature is increased from 700 °C 800 °C at 9 hrs 43 min and maintained till 13 hr 33min. H₂S is removed from the feed stream at 13 hrs 33 min and regeneration is continued till 19 hrs 32 min

also reconfirms the reproducibility of our experiments. Since chemisorption is exothermic an improved sulfur removal is naturally expected by increasing the temperature [2]. Higher temperature favors the kinetics for desorption reactions and recombination reactions involving adsorbed sulfur species. After reaching the steady state, H₂S is completely removed from the feed gas (all other gas flow rates remain the same) and the catalyst is allowed to regain its activity further. 92% of the activity is recovered by this process. This again corresponds very well with the final activity reported in Fig. 6 for 100 ppm case. The mole fractions of various gases from the reactor exit for the same case are shown in Fig. 10. At steady state before introducing H₂S into the reactor, CH₄ is fully converted and the reactor exit contains ~33% H₂, 9% CO, 9% CO₂ and remaining N₂. As soon as H₂S is introduced to the reactor, the reactants mole fraction starts to increase and the products mole fraction starts to decrease. The mole fraction of CH₄ and CO₂ increases and stabilizes respectively at 15% and 10%. These values corresponds very well to dry inlet mole fraction of CH₄ (16.7%) and CO₂ (11.2%). The 3% H₂ and 1.5% CO at the reactor exit is due to the residual activity (2%) of the catalyst.

3.5. Regeneration by steam treatment

Conventionally, the sulfur poisoned Ni is regenerated by sequential steam, steam air, and steam hydrogen treatment. Since the removal of adsorbed sulfur can be easily achieved

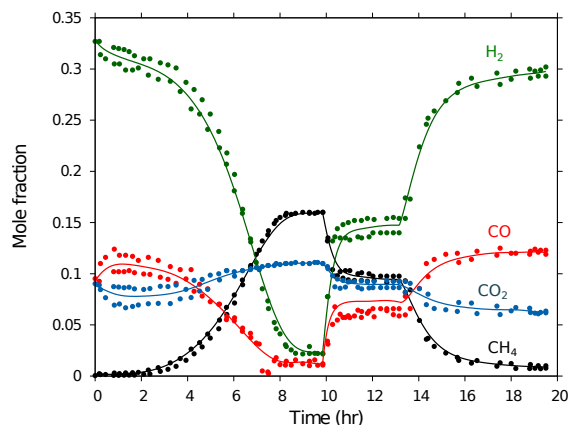


Figure 10: Mole fraction of various gases out of the reactor during the activity regeneration by temperature enhancement corresponding to Fig. 9.

by steaming above 650 °C [2] we have attempted the regeneration by treating with H₂O. Once the catalyst is fully deactivated at 700 °C, the feed stream is replaced with H₂O (48.08 ml min⁻¹) diluted in N₂ (102.4 ml min⁻¹) flow for ~5 h. Since steam treatment leads to the formation of NiO the catalyst is further reduced under H₂ flow (20 ml min⁻¹) at 700 °C for 5 h. Total regeneration time is 10 h, which is far shorter than the regeneration time reported by Li et al. and Nielsen [1, 2]. The regenerated catalyst is tested for its

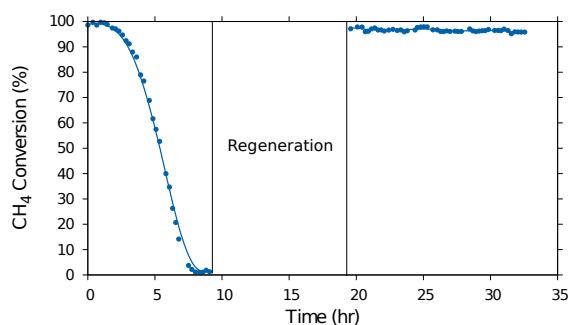


Figure 11: Regeneration of poisoned catalyst at 700 °C by steam treatment.

activity by performing reforming reaction without H₂S in the feed stream. CH₄ conversion after regeneration is shown in Fig 11. The catalyst showed stable operation for more than 10 hrs whereas Li et al. observed fall in activity of the catalyst regenerated using conventional sequential technique after 10 hrs of operation. Its very likely that the steam treatment regenerates the catalyst by forming SO₂. The oxygen atoms are formed by the dissociative adsorption of H₂O on Ni surface.

4. Conclusions

Ni Catalyst poisoning due to H₂S during the reforming of biogas is studied. The experiments are performed at 700 °C and 800 °C and for three different H₂S concentrations (20, 50, and 100 ppm w.r.t CH₄+CO₂ concentration). At 700 °C, the saturation sulfur coverage is independent of H₂S concentration

in the feed gas. However, at 800 °C, the saturation coverage of sulfur is dependent on the concentration of H₂S. Generally, higher H₂S concentrations lead to faster deactivation of the catalyst. The deactivation and regeneration showed exponential behavior on time on stream. At higher H₂S concentrations (50 and 100 ppm), the rate of deactivation is found to be independent of the temperature. At 800 °C, the activity of the catalyst is partially recovered just by removing H₂S from the feed gas. However, this method did not recover the catalyst activity at 700 °C. Regeneration of the poisoned catalyst at 700 °C required either temperature enhancement or steam treatment. The activity of the catalyst which is almost completely poisoned by exposure to 100 ppm H₂S at 700 °C is regenerated partially by enhancing the temperature to 800 °C and the catalyst is almost completely regenerated by removing H₂S from the feed gas. The same catalyst may also be regenerated by steam treatment. Five hours of steam treatment followed by reduction in H₂ for 5 hrs led to almost complete recovery of the catalyst activity. This regeneration time is far shorter than the ones reported in previous literature.

Acknowledgment

We acknowledge the funding received from DST under the project SR/RC-UK/Fuel-Cell-03/2011/IITH (G). We are thankful to Dr Debaprasad Shee (IITH, India) for the encouraging discussions and support.

- [1] Li L, Howard C, King DL., Gerber R, Dagle R, Stevens D, Regeneration of Sulfur Deactivated Ni-Based Biomass Syngas Cleaning Catalysts. *Ind. Eng. Chem. Res.* 2010;49:144–8.
- [2] Rostrup-nielsen JR, Some principles related to the regeneration of sulfur poisoned Nickel catalyst. *J. Catal.* 1971;178:171–8.
- [3] Izquierdo U, Barrio V, Requies J, Cambra J, Güemez M, Arias P, Tri-reforming: A new biogas process for synthesis gas and hydrogen production. *Int. J. of Hydrogen Energy.* 2012;38:1–9
- [4] Izquierdo U, Barrio V, Lago N, Requies J, Cambra J, Güemez M, Arias P, Biogas steam and oxidative reforming processes for synthesis gas and hydrogen production in conventional and microreactor reaction systems. *Int. J. of Hydrogen Energy.* 2012;37:13829–42.
- [5] Effendi A, Zhang Z, Hellgardt K, Honda K, Yoshida T, Steam reforming of a clean model biogas over Ni / Al₂O₃ in fluidized- and fixed-bed reactors. *Catal. Today.*2002;77:181–9.
- [6] Effendi A, Hellgardt K, Zhang Z, Yoshida T, Optimising H₂ production from model biogas via combined steam reforming and CO shift reactions. *Fuel.* 2005;84:869–74
- [7] Janardhanan VM, Deutschmann O, CFD analysis of a solid oxide fuel cell with internal reforming : Coupled interactions of transport, heterogeneous catalysis and electrochemical processes. *J. Power Sources.* 2006;162:1192-202. 1192–1202.
- [8] Thormann J, Maier L, Pfeifer P, Kunz U, Deutschmann O, Schubert K, Steam reforming of hexadecane over a Rh / CeO₂ catalyst in microchannels : Experimental and numerical investigation. *Int. J. Hydrogen Energy.*2009;34:5108–20.
- [9] Kolbitsch P, Pfeifer C, Hofbauer H, Catalytic steam reforming of model biogas. *Fuel.* 2008;87:701–6.
- [10] Lin KH, Chang HF, Chang ACC, Biogas reforming for hydrogen production over mesoporous Ni_{2x}Ce1 – xO₂ catalysts. *Int. J. of Hydrogen Energy.*2012;37:15696–703.
- [11] Oudar J, Sulfur Adsorption and Poisoning of Metallic Catalysts. *Catal. Rev. Sci. Eng.* 22. 1980;22:171–95
- [12] Bartholomew CH, Weatherbee DG, Jarvi GA, Sulfur Poisoning of Nickel Methanation Catalysts I. In situ Deactivation by H₂S of Nickel and Nickel Biometallics. *J. Catal.* 1979;60:257–69.
- [13] Ashrafi M, Pfeifer C, Pro T, Hofbauer H, Experimental Study of Model Biogas Catalytic Steam Reforming : 2 . Impact of Sulfur on the Deactivation and Regeneration of Ni-Based Catalysts. *Energy and Fuels.* 2008;22:4190–5. 4190–4195.
- [14] Rostrup-Nielsen JR, Chemisorption of Hydrogen Sulfide on a Supported Nickel Catalyst. *J. Catal.* 1968;227:220–7.
- [15] Erekson EJ, Bartholomew CH, Sulfur poisoning of Nickel methanation catalysts. *Applied Catalysis.* 1983;5:323–6.
- [16] Pannell RB, Chung KS, Bartholomew CH, The stoichiometry and poisoning by sulfur of hydrogen, oxygen and carbon monoxide chemisorption on unsupported nickel. *J. Catal.* 1977;347:340–7.
- [17] Özdemir H, Öksüzömer MF, Gürkaynak MA, Preparation and characterization of Ni based catalysts for the catalytic partial oxidation of methane: Effect of support basicity on H₂/CO ratio and carbon deposition. *Int. J. of Hydrogen Energy.* 2010;35:12147-60
- [18] Kuhn JN, Lakshminarayanan N, Ozkan US, Effect of hydrogen sulfide on the catalytic activity of Ni-YSZ cermets. *J. Molecular Catal.* 2008;282:9-21.
- [19] Deutschmann O, Tischer S, Janardhanan, VM, Correa C, Chatterjee D, Mladenov N, Minh HD, DETCHEM User manual. 2007

Table 1: BET Analysis of catalyst samples before and after experiments

Sample	BET Surface Area (m ² g ⁻¹)	Pore Volume (cm ³ g ⁻¹)	Average Pore Size (nm)
γ -Al ₂ O ₃	206	0.793	11.34
Calcined Ni/ γ -Al ₂ O ₃	151	0.626	12.09
Reduced Ni/ γ -Al ₂ O ₃	106	0.585	17.3
Spent catalyst after stability test at 800 °C	86	0.581	21.11
Spent catalyst at 700 °C	76	0.433	17.66

Table 2: Comparison between equilibrium prediction and experiments

Reactants/Products	Equilibrium		Experiments	
	800 °C	700 °C	800 °C	700 °C
CH ₄ Conversion (%)	99.86	98.08	99.7	97.75
CO ₂ Conversion (%)	22.85	7.03	23.2	5.6
H ₂ dry molefraction (%)	32.23	32.6	31.0	31.0
CO dry molefraction (%)	13.06	11.5	13.0	11.3